Int. J. Heat Mass Transfer. Vol. 17, pp. 1571–1589. Pergamon Press 1974. Printed in Great Britain

ECLECTIC MERGER OF CROCCO–LEES AND CHAPMAN–KORST APPROACH TO NEAR WAKE*

JIMMIE H. SMITH
Sandia Laboratories, Division 1543, Albuquerque, New Mexico, U.S.A.

and

J. PARKER LAMB
Department of Mechanical Engineering, The University of Texas at Austin, Texas, U.S.A.

(*Received* 26 *November* 1973 *and in revised form* 20 *March* 1974)

Abstract—In addition to reviewing the two classical approaches, the supersonic ($1{\cdot}5 \leqslant M_\infty \leqslant 5$) turbulent planar base flow problem is solved in a novel manner with integral techniques. The heretofore separate branches of effort stemming from the Chapman–Korst component analysis and the Crocco–Lees critical point method are merged. The dichotomy is ended by using the Chapman–Korst component analysis to establish all flow parameters in terms of assumed values of base pressure. A final closure is then obtained by using two interpretations of the Crocco–Lees critical point theory to select the correct base pressure along with corresponding parameters of interest. The fact that the prediction methods as well as extensive experimental data are in close agreement provides substantial confirmation of the new methods.

NOMENCLATURE

B, dimensionless reverse flow width, b/b_r;
b, reverse flow half-width;
C, Crocco number, $u/(2C_pT_0)^{1/2}$;
TR, temperature ratio, $T/T_0 = 1-C^2$;
h, base half height;
K, eddy viscosity constant;
L, length of free mixing zone;
M, Mach number;
P, P_0, static and stagnation pressure;
T, T_0, static and stagnation temperature;
$\dot{m}$, mass flux;
$\dot{M}$, momentum flux;
$\dot{M}E$, mechanical energy flux;
S, distance from base;
u, v, shear layer velocities in x and y directions;
x, y, coordinates for viscous layer;
$\tilde{x}, \tilde{y}$, reverse flow coordinates;
$\tilde{u}$, reverse flow velocity in $\tilde{x}$-direction;
$\bar{u}$, flow velocity at reattachment;
$\hat{u}$, $\bar{u}$ after compressibility transform;
α, reattachment angle;
γ, ratio of specific heats, C_p/C_v;
δ, layer thickness;
δ^*, displacement thickness;
δ_t, throat width of hypothetical converging–diverging nozzle;
Ψ, viscous dissipation;
ζ, dimensionless ratio for reverse flow, $\tilde{y}/b$;
z, dimensionless boundary-layer ratio, $\bar{y}/\delta$;
η, similarity variable for shear layer, $\sigma y/x$;
σ, shear layer spread rate parameter;
τ, shear stress;
ρ, density;
θ, flow angle;
Λ, stagnation temperature ratio in shear layer, T_0/T_{02};
$\tilde{\Lambda}$, stagnation temperature ratio in reverse flow, T_0/T_{0r};
Λ_w, stagnation temperature ratio in reattaching layer, T_0/T_{0w};
λ_b, stagnation temperature ratio across shear layer, T_b/T_{02};
$\tilde{\lambda}_b$, stagnation temperature ratio across reverse flow, T_b/T_{0r};
λ_r, stagnation temperature ratio between free stream and reverse flow $\mathcal{L}$, T_{0r}/T_{02};
λ_w, stagnation temperature ratio between wall and free stream, T_{0w}/T_{02};
Φ, velocity ratio, $\tilde{u}_{\mathcal{L}}/\tilde{u}_r$;
$\tilde{\varphi}$, velocity ratio, $\tilde{u}/\tilde{u}_{\mathcal{L}}$;
φ, velocity ratio, u/u_2;
$\bar{\varphi}$, velocity ratio, $\bar{u}/\bar{u}_w$.

Subscripts

B, evaluation at $\mathcal{L}$ of base plane;
b, evaluation on zero velocity streamline at interface station;

*This work was done under the auspices of the United States Atomic Energy Commission and is taken from the first author's Ph.D. dissertation.

$\underline{\varphi}$, evaluation on $\underline{\varphi}$ of reverse flow;
0, evaluation at lower edge of free shear layer;
j, evaluation on dividing streamline in free shear layer;
m, evaluation in reverse flow where $\tilde{\varphi} = 0{\cdot}5$;
0, evaluation for isentropic stagnation conditions;
e, evaluation at outer edge of free shear layer;
r, evaluation at $\underline{\varphi}$ of reverse flow and interface station;
w, evaluation at reattachment point;
2, evaluation in free stream adjacent to mixing region;
1, evaluation in free stream of approach flow;
i, inviscid quantity;
v, viscous quantity.

List of integrals

$$I_{1x} = \int_{-\infty}^{\eta_x} \frac{\varphi \, d\eta}{\Lambda - C_2^2 \varphi^2};$$

$$I_{2x} = \int_{-\infty}^{\eta_x} \frac{\varphi^2 \, d\eta}{\Lambda - C_2^2 \varphi^2};$$

$$J_1 = \int_0^1 \frac{\tilde{\varphi} \, d\zeta}{\tilde{\Lambda} . TR};$$

$$J_2 = \int_0^1 \frac{\tilde{\varphi}^2 \, d\zeta}{\tilde{\Lambda} . TR};$$

$$J_3 = \int_0^1 \frac{\tilde{\varphi}^3 \, d\zeta}{\tilde{\Lambda} . TR};$$

$$J_5 = -\int_0^1 \frac{\tilde{\varphi}^3 \, d\zeta}{(\tilde{\Lambda} . TR)^2};$$

$$J_6 = -\int_0^1 \frac{\varphi^2 \, d\zeta}{(\tilde{\Lambda} . TR)^2};$$

$$J_7 = \int_0^1 \frac{\tilde{\varphi}^4 \, d\zeta}{(\tilde{\Lambda} . TR)^2};$$

$$\hat{I}_{1e} = \int_0^1 \frac{P}{P_e} \frac{\hat{\varphi} \, dz}{\Lambda - C_e^2 \hat{\varphi}^2}.$$

Note: J_{nm} is J_n with upper limit on integral changed to ζ_m.
J_{nr} is J_n evaluated at interface station.

INTRODUCTION

1.1. *Origin of the present problem*

THE SUPERSONIC turbulent planar base flow problem is still an important problem area after two decades of effort. This longevity is indicative of the degree of difficulty of the problem. The importance stems from the dual necessities of predicting base drag and heat transfer for flight vehicles. In the high hypersonic regime, skin friction drag dominates the much smaller wave drag. By contrast, in the supersonic regime of the present study, wave drag is of comparable magnitude to skin drag and cannot be ignored.

High local heating rates occur at reattachment of separated flows and at the centerline of the base-region reverse flow. Large surface protuberances, surfaces with a small radius of curvature, or adverse pressure gradients may cause separation. Base flows or wakes are found on the lee side of blunt trailing edges whether they are on protuberances, wings, or other bodies. In such situations, a necessary first step in computing drag or heating in the base region is the establishment of the base flowfield which is characterized by the base static pressure. This latter parameter is determined largely by the amount of turbulent mixing between the outer inviscid and inner viscous layers.

1.2. *General description of flow patterns*

Figure 1 illustrates the geometry and flow components of the present study. The expansion at the corner of a backstep or base of a blunt body may be approximated by simple Prandtl–Meyer theory. The expanding flow turns the corner and clings to the base for a short distance (order of $h/10$) before separating. Experiments indicate that the flow actually overexpands and then recompresses with a lip shock to the pressure which global flow conditions can sustain [1]. The base region static pressure, P_b, is considerably lower than the approach pressure, P_1. The ratio of base to approach static pressure ranges from one-half at Mach 1·5, to one-tenth at Mach 5. Near the downstream wall or plane of symmetry, the mixing layer interacts with the reverse flow entering the base region. The beginning of this interaction serves as a demarcation line or interface between the isobaric base region and the recompression zone. The interaction between forward and reverse flows initiates a recompression which is characterized by a nearly linear rise in static pressure.

At the reattachment point of the dividing streamline, a local stagnation process occurs. The dividing streamline by definition, separates the flow into two parts; namely, (1) those streamlines possessing enough kinetic energy to overcome the adverse pressure gradient and proceed downstream, and (2) those streamlines which are reversed back toward the base by the unfavorable gradient.

Outside the viscous layer near the reattachment of the dividing streamline there is a coalescence of Mach lines to form a recompression shock. This shock may interact with the lip shock described earlier to produce expansion waves which affect the redeveloping layer by slowing its rate of recovery of the approach pressure.

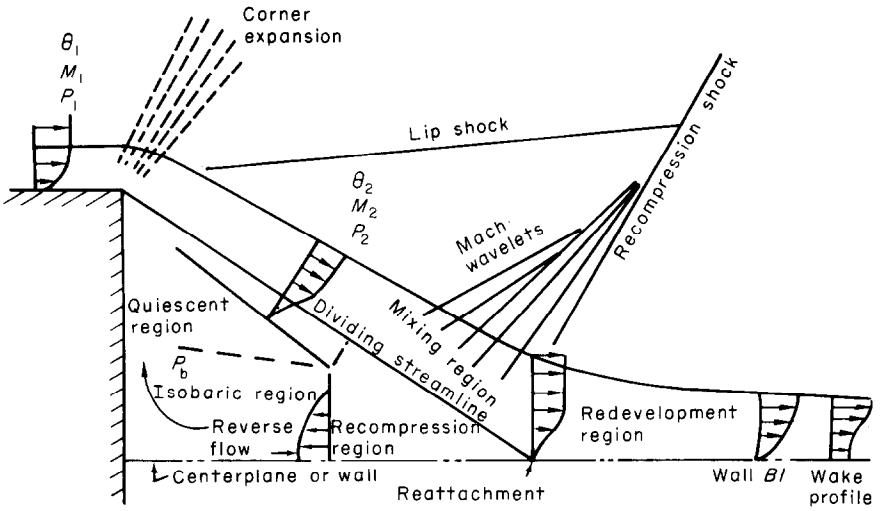

FIG. 1. Flow components in supersonic turbulent near wake.

1.3. *The two classic approaches*

1.3.1. *Historical developments.* Pioneering predictions of base flow resulted in the initiation of two distinct branches of continuing effort. One branch began with Chapman [2] and Korst [3] who developed expedient solutions which do not entail great complexity. Chapman correlated laminar flow base pressure data with δ/h where δ is the usual upstream boundary-layer thickness and h is the base height although a rationale for this correlation has never been found. Both Chapman (for laminar flow) and Korst (for turbulent flow) proposed an escape criterion for the dividing streamline based upon isentropic flow. The fundamental assumptions of this escape criterion are known to be invalid yet the resulting base pressure predictions are remarkably good.

Another branch of analysis began with Crocco and Lees [4] who cautioned that to neglect the strong viscous–inviscid interaction in such flows is fundamentally incorrect. They stressed the importance of mixing in high speed flow just as did Schubauer and Klebanoff [5] in low speed flow. The key concept in the Crocco–Lees approach is that the inviscid solution for the external flow must be carried out simultaneously with an inner viscous solution.

Although many design problems tend to deal with three-dimensional interactions for which even the inviscid solution is not well known, Korkegi [6] has stressed that simpler situations such as the present planar turbulent supersonic base flow must be thoroughly understood if one is to have any hope of predicting effects in the more complex situations. Furthermore Hunter and Reeves [7] have pointed out that "only slight modification of basic two-dimensional theory leads to reliable calculations of the separated flow field for practical control configurations which, up to now, have been analyzed by using correlations of experimental data".

The main disadvantage of the Crocco–Lees or critical point approach is the detailed empirical input required. Such initial data are not generally known. Also, flow models using this approach require complex iterative solutions and excessive computer time. These features have prevented widespread engineering usage although, once the deficiencies are accepted, a wealth of flow details can be predicted.

The Chapman–Korst or component approach also has some deficiencies. Other than the already mentioned dubious assumptions concerning the isentropic escape criterion, there are other defects such as those summarized by Alber and Lees [8]. They criticize the work of Korst [3], Nash [9], and McDonald [10] for treating the recompression process in a "black box" manner in order to predict base pressure. They further claim that these theories are incapable of predicting important near-wake characteristics such as length of recompression, rear stagnation point, reattaching layer growth rate, and longitudinal pressure variation near reattachment. They point out quite rightly that omission of the strong viscous–inviscid interaction is often the major deficiency in a component analysis.

In previous prediction techniques, there has been a tendency to make a binary choice between the two pioneering approaches. An eclectic approach would seem to offer considerable improvement in our general prediction capability. That is, the considerable merits of each approach can be merged in a method such as that proposed herein which overcomes in an approximate manner each objection noted above.

1.3.2. *Crocco–Lees model.* A number of investigators have applied the Crocco–Lees critical point theory to laminar flows, but few have attempted to extend the prediction method to turbulent base flows. However, a number of the developments in laminar flow can be carried over to the turbulent case. Webb, Golik, Vogenitz and Lees [11] and Reeves and Lees [12] used integral moments of the boundary layer equations while Baum [13] and Baum and Denison [14] applied finite difference methods. For integral methods, global assumptions suffice while difference methods require detailed local assumptions which unfortunately cannot be based soundly on experiment because of sparse data.

Investigators such as Baum and Denison [14], Webb, Golik, Vogenitz and Lees [11] and Alber and Lees [8] identify true base pressure as that which allows the solution to progress farthest downstream without a contradiction like a negative displacement thickness. To proceed past the critical point, they restart their calculations with parameters obtained upstream of the critical point. Other variants of the critical point are:

(a) the point at which the angle θ_e induced at the edge of the inner viscous layer as identified by integral continuity equals the outer inviscid flow angle, $\tan^{-1}(v/u)_e$,

(b) the point at which $\mathrm{d}\delta/\mathrm{d}p = 0$,

(c) the point at which

$$\int_0^\delta \frac{1-M^2}{M^2}\,\mathrm{d}y = 0,$$

(d) the point at which $\theta = \tan^{-1}(v/u)_e$, becomes insensitive to $\mathrm{d}p/\mathrm{d}\delta$.

Regardless of method, the critical point is a saddle point singularity downstream of the rear stagnation point. Solutions which do not pass through this critical point exhibit unrealistic behavior. The spurious solutions are sometimes indicated by centerline velocities which increase or decrease unrealistically as seen in Shamroth and McDonald [15].

Classical boundary-layer theory assumes that the external pressure is impressed through the layer. Although this principle has often been applied to base flows, Weiss and Weinbaum [16] warn of the importance of accounting for transverse gradients at high Mach numbers. Holden [17] points out that Reeves and Lees [12] forced the subcritical to supercritical jump on themselves by ignoring transverse pressure gradients. Crocco [18] originated the concepts of subcritical and supercritical flow to help match mathematical simulations to actual boundary layer behavior. He defined a subcritical boundary layer as one in which δ^* (or δ) would increase in an adverse pressure gradient and conversely for a supercritical layer. One may also think of subcritical flow as being subsonic in the mean and supercritical flow as being supersonic in the mean. Table 1 gives a summary of the main developments in Crocco–Lees prediction methods.

1.3.3. *Chapman–Korst analyses.* Since the advent of the Chapman–Korst base flow analysis, it has been subjected to continuing criticism for its apparent lack of rigor even though it is simple to use and the resulting predictions of base pressure agree very well with experimental data. A large amount of effort has been devoted to extending the theory to account for transverse pressure gradients, upstream boundary layer, and other refinements.

However, Baum and Denison [14] believe that accounting for transverse pressure gradients complicates integral methods to such an extent that they may no longer be simpler than finite difference methods. If done in certain ways, their fear could almost be justified. In the present work transverse pressure gradients are accounted for in an approximate way. Yet a complete base flow analysis requires only 5–10 s on the CDC 6600. Current finite difference methods often require double precision and take up to 30 min on this same machine.

Many investigators find it necessary to account for the upstream boundary layer and its effect on the mixing layer. This effect destroys initial profile similarity in the mixing zone and of course ultimately affects the base pressure. Kirk [19] devised an origin shift technique to account for this effect while Roberts [20] used Kirk's origin shift idea plus some suggestions by McDonald [10] to improve his predictions at reattachment. Nash [9] showed that difficulties in extending the Chapman–Korst component analysis stem from the simple recompression model. To alleviate the difficulty, he proposed a constant $N = 0{\cdot}35$ for the fraction of dividing streamline isentropic stagnation pressure recovered at the wake stagnation point. Cooke [21] obtained improved results with $N = 0{\cdot}5$ while McDonald [10] and others showed clearly that no constant value was satisfactory as N should be a function of Mach number. Nash himself has since retracted his constant-N suggestion.

A case may be made for ignoring the upstream boundary layer. Correlation of surface pressure data by Wu, Su and Scherberg [22] indicates that the sonic line is very close to the corner, effectively blocking most upstream communication. Smith [23] concludes that base pressure is a strong function of approach boundary layer in transitional flows but only weakly related in fully turbulent flows such as the present. Finally, Hasting [24] shows that base pressure is not perturbed significantly by upstream boundary layers of less than half the step height ($\delta \leqslant \frac{1}{2}h$). In view of this preponderance of evidence, it is considered unnecessary to apply Kirk's [19] origin shift as did Nash [9].

Table 1. Chronology of Crocco–Lees critical point analyses of base flow

Year	Predictor and reference	Major features
1952	Crocco and Lees [4]	Emphasizes mixing interaction between external inviscid flow and inner dissipative flow. Derives critical point of equation and explains it as analogous to flow through nozzle throat. Uses empirical relations to get certain unknowns. Laminar and turbulent flow.
1965	Reeves and Lees [12]	Modifies and improves Crocco–Lees theory and removes empiricism. Ignores transverse pressure gradients. Laminar flow.
1965	Webb *et al.* [11]	Introduces multimoment integral methods in rigorous application of Crocco–Lees critical point theory. Improves prediction of pressure recovery distance. Laminar flow.
1967	Baum and Denison [14]	Rigorous and time consuming application of finite difference methods to critical point theory. Laminar flow.
1968	Weinbaum and Garvine [61]	Identifies two critical points, one realistic. Elaborates on the one-dimensional inviscid throat and a two-dimensional viscous analogy.
1968	Alber and Lees [8]	Extends Reeves and Lees model to supersonic turbulent base flows. Includes eddy viscosity and compressibility transform.
1969	Holden [17]	Demonstrates that slight transverse pressure gradient eliminates need for subcritical–supercritical jump encountered by Reeves and Lees.
1970	Ai [60]	Mathematical examination of singularities or critical points per se. Clarifies anomolous details in Webb *et al.* [11]. Laminar flow.
1970	Shamroth and McDonald [15]	Extends Crocco–Lees strong interaction model by including transverse momentum integral equation. Turbulent but applicable to laminar flow.
1971	Hunter and Reeves [7]	Defines short and infinite ramp flows wherein the critical point may occur upstream or downstream of trailing edge. Turbulent flow.
1973	Smith [41]	Uses Chapman–Korst component analysis combined with Crocco–Lees critical point for closure.

Another point of contention concerns the proper interpretation of the Chapman–Korst escape criterion. Many observers object that the escape criterion is based on isentropic flow when in reality it is applied to the dividing streamline near stagnation where the flow is clearly irreversible and diabatic. Hood [25] and Lamb and Hood [26] take the view that Korst did not mean to imply actual isentropic flow. Lamb and Hood [26] affirm the validity of the escape criterion with the proper interpretation.

Nash interpreted Korst's recompression hypothesis to mean that the flow along the dividing streamline actually undergoes isentropic recompression to the final downstream pressure at reattachment. In reality, the reattachment pressure is only about half the final downstream pressure. Korst contributed to this misconception by showing that flow along streamlines near the velocity profile inflection point is in the first approximation isentropic although actually irreversible diabatic. According to Hood, Korst should have explicitly stated that the dividing streamline is above this inflection point at the beginning of recompression and well below it at reattachment. Table 2 summarizes developments in the Chapman–Korst method of analysis.

1.4. *Introduction to the present formulation*

Turbulent boundary layers are characterized by strong dependence on Mach number but weak dependence on heat transfer and Reynolds number [27–29]. The weak dependence of the flowfield on heat transfer allows one to uncouple the energy equation from the motion equations. With this simplification one can establish the flowfield first and subsequently extend the predictions to include heat transfer in the fashion of Korst [30] and Lamb and Hood [26]. The present effort will stress primarily the simplified modeling of a real flow while retaining engineering accuracy in all desired flow parameters.

As shown in Fig. 1, the viscous flow region bounded by the baseplane, the centerplane, and the dividing streamline will be analyzed by using two control volumes as did Greenwood [31]. One control volume extends from the baseplane to the beginning of recompression and includes all of the isobaric flow. The other control volume extends from the interface between the two control volumes to the point of dividing streamline reattachment (or wake stagnation point). At this point, one has the flow below the dividing streamline established entirely through a component or Chapman–Korst type of analysis. That is,

Table 2. Chronology of Chapman–Korst component analyses of base flow

Year	Predictor and reference	Major features
1950	Chapman [2]	Uses detailed analytical studies of various flow components, merges the results to account for interaction between components. Empirical data used to get base pressure. Laminar flow.
1955–1956	Korst, Page and Childs [62] and Korst [3]	Uses Chapman analysis but adds escape criterion to predict P_b. Turbulent flow.
1957	Chapman, Kuehn and Larson [63]	Uses component analysis and emphasizes dividing streamline and transition. Laminar and turbulent flow.
1959	Kirk [19]	Conceives origin shift to account for upstream boundary layer.
1962	Nash [9]	Two-dimensional turbulent base flow using Kirk's origin shift and suggesting a constant fraction ($N = 0{\cdot}35$) for pressure recovery at reattachment.
1963	Page and Dixon [64]	Component analysis with reflected image technique for heat transfer. Turbulent flow.
1964	McDonald [10]	Emphasizes importance of reattachment in determining P_b. Predicts but fails to measure strong Re-effect on P_b. Disproves Nash's constant recovery fraction. Turbulent flow.
1965	Greenwood [65]	Uses Chapman–Korst analysis plus Page and Dixon reflected image for heat transfer, adds mass injection. Turbulent flow.
1965	Korst [30]	Adds thermal and mechanical energy considerations to usual component analysis. Turbulent flow.
1966	Roberts [20]	Combines Kirk's virtual origin with McDonald's improvements on reattachment. Turbulent flow.
1966	Childs, Paynter and Redeker [34]	Uses longitudinal and transverse momentum equations in recompression zone control volume. Turbulent flow.
1967	Page, Kessler and Hill [36]	Emphasizes reattachment, uses empirical correlations for reattachment pressure. Turbulent flow.
1970	Lamb, Hood and Johnson [47]	Uses Chapman–Korst analysis but adds mass injection, heat transfer, compressibility. Turbulent flow.
1971	Greenwood [31]	Chapman–Korst flow analysis but replaces Korst escape criterion with matching of viscous and inviscid δ^*'s to select P_b. Turbulent flow.
1973	Smith [41]	Uses Chapman–Korst component analysis combined with Crocco–Lees critical point for closure.

one has values for each flow property of interest for each assumed value of base pressure.

To select the correct base pressure or close the overall analysis, a strong viscous–inviscid interaction criterion which uniquely determines the base pressure is used. A major purpose of the present study is to present several closure models and allow their merits to be determined by comparisons to experimental data. Specifically four base pressure prediction schemes will be employed. One is the Chapman–Korst method which is carried along as a fiducial while the second is a modification of the model proposed by Greenwood [31] which determines the correct base pressure by matching inviscid and viscous predictions of displacement thickness at reattachment.

In addition, two entirely new base pressure prediction methods are proposed; both are based on the Crocco–Lees critical point theory. More specifically, they are based on a broader interpretation of the downstream throat analogy which was originally proposed as an aid in understanding the critical point theory. To help explain this concept, Crocco and Lees pointed out that the critical point is analogous to the throat of a converging–diverging nozzle. In the current models, this analogy with a one-dimensional converging–diverging nozzle is assumed to be literally true. Since such nozzles have a minimum area at the throat, one of the proposed methods determines the correct base pressure by matching the viscous and inviscid estimates of minimum flow area downstream of reattachment.

The nozzle hypothesis rules out entrainment which as will develop later is quite significant. Another nozzle characteristic is that the variation of mass flux per unit area has a stationary point at the throat. This feature furnishes another possible closure criterion for base pressure determination. The last two closure criteria, while admittedly heuristic, are shown to be simple to use and quite effective.

Since the base region (or near wake) receives the primary thrust of this current effort, the hypothetical downstream throat marks the end of the analysis. Thus the lengthy and time consuming iteration about

the critical point as foreseen by Shamroth and McDonald [15] is not required.

Many experimental results, for example those of Roshko and Thomke [32] and Hama [1], serve as a basis for the current approximations such as isobaric mixing near the base, a straight dividing streamline trajectory for planar flow, and a linear pressure gradient from the beginning of recompression to reattachment.

The constrained reverse jet is sufficiently different from the usual free jet that negligible entrainment occurs. An innovation* in the present work is the use of continuity in addition to the usual conservation of momentum to govern the reverse flow. Both Hood [25] and Johnson [33] failed to distinguish between this constrained reverse flow and the usual free jet.

The use of longitudinal and transverse momentum equations in the recompression region (CV-II) is similar to earlier works by Childs, Paynter and Redeker [34] and Kessler and Page [35]. Korst [3] used an oblique shock to reach downstream static pressure. The present work uses isentropic inviscid turning until the flow is again parallel to the wall or centerplane.

The present work follows Page, Hill and Kessler [36] among others in the use of isobaric flow from the base to the cutoff station. The present study deals only with the so-called "infinite ramp" solutions of Hunter and Reeves [7]. In this case, the subcritical–supercritical transition would be expected at the critical point which marks the terminal point of the analysis. Since the flow downstream of this transition is unable to communicate with the upstream region of interest here, one may safely ignore it. Thus a lengthy and time consuming iteration starting at the critical point and marching in both directions as foreseen by Shamroth and McDonald [15] is not necessary here.

Some observers such as Stollery and Hankey [37] believe that an arbitrary choice of mathematical formulation leads fortuitously to surfaces along which gradients of flow parameters become infinite. Thus they claim that the critical boundary is a mathematical quirk devoid of physical significance. An overwhelming multitude of investigators, using methods as diverse as integral and finite difference solutions, find the critical point meaningful. The present study also finds conclusive evidence of the existence of a valid critical point, as will be seen in the results section. Physical significance is almost assured by the close agreement between predictions using critical point theory and corresponding experimental data. To clinch the physical existence of a critical point, direct experimental confirmation was obtained by Carriere (Reference 5 in Alber and Lees [8]).

*Communicated to Greenwood [31] for inclusion in his dissertation.

The length of shear layer is a critical parameter because it determines the surface area through which momentum and shear work are transferred from the external stream. In essence, the length of shear layer determines the base pressure which the flow will support. On the basis of dividing streamline arguments, Erdos and Pallone [38] conclude that the length of separated flow depends upon the reattachment pressure rise. This is similar to the judgement of Nash [9] and others that the reattachment physics are crucial to the prediction of P_b.

Shamroth and McDonald [15] point out that in regions where the mean flow field and turbulence structure change slowly with distance, accurate predictions are feasible with a simple eddy viscosity or mixing length model which assumes a unique relationship with turbulent local mean velocity. However in the near wake recompression region, predictions of this type would not be accurate. In the present model an eddy viscosity is used to describe the slowly changing reverse flow from the beginning of recompression back to the base. However no attempt is made to describe the flow inside the recompression zone. Instead only fluxes across surfaces of a control volume bounding this region are dealt with.

2. FLOW COMPONENTS AND GOVERNING EQUATIONS

2.1. *Corner flow*

Hama [1] has demonstrated that the boundary layer does not separate from the upper surface of the body. Rather it overexpands around the corner, clinging to the base for a short distance (order of $h/10$) before separating from the base itself. To further complicate the flow, overexpansion is followed by an oblique lip shock which extends from near the corner through the shear layer and out into the free stream. Fortunately, the effects of this lip shock are minimal at free stream Mach numbers below 2. At higher Mach numbers, the effects of the lip shock can be accounted for, if necessary, by a final empirical geometric correction as shown by Lamb and Hood [39]. Another fortunate circumstance keeps the lip shock from seriously complicating the present analysis. Even at higher Mach numbers (up to 5) where the lip shock is embedded in the shear layer, it lies outside the dividing streamline. Both control volumes used in the present analysis lie inside the dividing streamline. The data of Roshko and Thomke [32] substantiate the present postulation that the complex corner flow does not significantly affect the interior of the near wake. With these justifications, a simple Prandtl–Meyer expansion [40] was used around the corner as detailed in Smith [41].

2.2. *Spread rate parameter for free turbulent shear layer*

Shear layer spread rate models of Lamb [42], Gaddis [43], Bauer [44], and Channapragada and Wooley [45] were investigated during the current study. The only unanimity in the literature on this subject is that σ increases with Mach number. The Bauer-σ was selected as the best phenomenological model because of its dependence on the velocity, location and shear stress along the very important dividing streamline, a dependence which the other models lacked. Bauer's σ is given by.

$$\sigma = \frac{\pi\sigma_0}{0{\cdot}5085}(1-C_2^2\varphi_j^2)I_{2j} \tag{1}$$

where the incompressible spread rate is given by $\sigma_0 = 12$.

2.3. *Free turbulent shear layer analysis*

The well-known basic analysis by Korst [3, 30, 26, 31, 46, 47, 41] is used to describe the shear layer in the isobaric region and locate the dividing streamline. In essence, Korst began with a motion equation plus highly restrictive boundary and initial conditions to which he applied Oseen linearization in order to reach a form of the diffusion equation whose solution is,

$$\varphi = \frac{u}{u_2} = \tfrac{1}{2}(1+\operatorname{erf}\eta) \tag{2}$$

where $\eta = \sigma\, y/x$ is a similarity parameter.

To account for the approximations inherent in the boundary and initial conditions, Korst determines a shift parameter, η_m, which balances the momentum.

2.4. *Transverse pressure gradient at reattachment*

Classical boundary-layer theory postulates a small transverse dimension compared with longitudinal variation. Additionally, free stream pressure is assumed to be impressed uniformly through the layer. However, in relation to the current separated flow field, Weiss and Weinbaum [16] and Baum and Denison [14] point out that at high Mach numbers the viscous flow field may contain non-negligible transverse pressure gradients. In the present study, predictions of base pressure were improved after incorporating the pressure variation across the reattaching layer.

Initially, a transverse pressure variation based on a linearized velocity equation [48] was derived,

$$P_e = P_w - \delta_w\beta_w\left(\frac{\partial P}{\partial x}\right)_w \tag{3}$$

where $\beta_w = \sqrt{(M_w^2-1)}$.

Unfortunately this purely analytical approach did not yield base pressure predictions which were in close agreement with experimental data. It was therefore necessary to introduce,

$$P_e = P_2 + \left(1 - \frac{S_{re}-S_r}{S_w-S_r}\right)(P_w-P_2) \tag{4}$$

which is based on the data of Chow's Fig. 5 [49].

2.5. *Reattachment profile*

The Karman–Pohlhausen separation profile [50] with shape factor $Q = -12$ is,

$$\bar{\varphi} = \frac{\bar{u}}{u_e} = z^2(6-8z+3z^2) \tag{5}$$

where $0 \leqslant \bar{y}/\delta = z \leqslant 1$.

This profile is quite good for low Mach numbers of about 2. However for higher Mach numbers where compressibility is more significant, a compressibility transform developed by Maise and McDonald [51] is,

$$\hat{\varphi} = \frac{1}{C_e}\sin\left[C_e(\bar{\varphi}-1)+\operatorname{Arcsin}C_e\right]. \tag{6}$$

This equation employs the Van Driest generalized velocity in the form,

$$\frac{u^*}{u_e} = \frac{1}{C_e}\operatorname{Arcsin}C_e\bar{\varphi}. \tag{7}$$

2.6. *Reverse flow*

A three parameter family, $\tilde{\varphi}$, ϕ and B, each defined in the Nomenclature, will be used to describe the spreading and velocity decay of the reverse flow. A simple relationship exists between φ for the shear layer and these new velocity ratios.

$$\varphi = \frac{u}{u_2} = \frac{u}{u_{\varrho}}\frac{u_{\varrho}}{u_{\varrho r}}\frac{u_{\varrho r}}{u_2} = \tilde{\varphi}\phi\frac{u_{\varrho r}}{u_2} \tag{8}$$

but at the interface station, $\phi \equiv u_{\varrho}/u_{\varrho r} \equiv 1$, so

$$\varphi = \tilde{\varphi}\frac{u_{\varrho r}}{u_2}(\text{general}) \tag{8a}$$

and for isoenergetic flow

$$\varphi = \tilde{\varphi}\frac{C_r}{C_2}(\text{constant } T_0) \tag{8b}$$

In actual flow patterns, the reverse flow velocity is relatively low and the development distance is short, thus the growth of the layer is minimal. For example, at Mach 5 the viscous reverse flow spreads about 14 per cent ($B_b = 1{\cdot}14$) by the time it reaches the base. At lower Mach numbers, the spread decreases until it reaches about 8 per cent at Mach 1·5.

Most literature dealing with two-dimensional turbulent jets [50, 52, 53] is strictly applicable only to

unconfined free jets which are able to entrain considerable mass from their quiescent surroundings. In the base region the reverse jet is not free, but is constrained by the surrounding isobaric region, and is much more turbulent than the usual free jet emanating from a hypothetical slit. The increased turbulence stems from its origin in the turbulent mixing layer before flow reversal in the rising pressure region. Thus when the usual free jet momentum equations for the overall flow and a central core bounded by $\tilde{\varphi} = 1/2$ were used with the present confined flow, the base pressure predictions did not agree closely with experiment. An examination of the closed recirculating flow loop makes it evident that, in the steady state, mass must be conserved. The use of continuity along with the usual core momentum equations gave significantly improved predictions. The profile equation will supply $\tilde{\varphi}$ while sequential simultaneous solutions of overall mass and core momentum in a forward marching procedure will supply ϕ and B. A profile equation which agrees with experimental data [52] is,

$$\tilde{\varphi} = \frac{\tilde{u}}{\tilde{u}_{\ell}} = \frac{\cos(\pi\zeta)+1}{2} \tag{9}$$

where $\zeta = \tilde{y}/b$ and $0 \leqslant \zeta \leqslant 1$.

After normalizing by $(\tilde{\rho}_{\ell}\,\tilde{u}_{\ell})_r$ and using Crocco's solution to the energy equation to relate temperature and velocity profiles, the overall reverse flow continuity relation may be written as,

$$\frac{1}{B}\cdot B' + \frac{1}{\phi} + \left[(1-\tilde{\lambda}_b)\frac{J_6}{J_1} - 2C_r^2\phi\frac{J^5}{J_1}\right]\phi' = 0 \tag{10}$$

J_1, J_5 and J_6 are defined in the Nomenclature.

A similar normalization of the core $(0 \leqslant \zeta \leqslant \frac{1}{2})$ momentum equation yields

$$\begin{aligned}&\phi^2(J_{2m}-J_{1m}/2)B' + \\ &+\{B\phi(2J_{2m}-J_{1m}/2)+B\phi^2[(1-\tilde{\lambda}_b)J_{5m}+2C_r^2\phi J_{7m} \\ &-(1-\tilde{\lambda}_b)J_{6m}/2+C_r^2\phi J_{5m}]\}\phi' = -\frac{\pi}{6}\frac{K\phi^2}{(\tilde{\lambda}-TR)_m}\end{aligned} \tag{11}$$

where

$$K = 0{\cdot}0055(1+\mathrm{e}^{-4C_r^2}). \tag{12}$$

The eddy viscosity constant, K, is taken from Peters [54] since his work deals with bounded turbulent jets as does the present work.

2.7. *Control volume I (CV-I)*

2.7.1. *Continuity for CV-I.* Mass entering the isobaric region of CV-I through the reverse flow may be expressed as,

$$\dot{m}_{\text{in}} = \int_0^{b_r}\tilde{\rho}\tilde{u}\,\mathrm{d}\tilde{y} = b_r\tilde{\rho}_r\tilde{u}_r\int_0^1\frac{\tilde{\rho}}{\tilde{\rho}_r}\frac{\tilde{u}}{\tilde{u}_r}\mathrm{d}Z = b_r\tilde{\rho}_r\tilde{u}_r(1-C_r^2)J_{1r}. \tag{13}$$

The mass flux leaving CV-I through the shear layer may be expressed as,

$$\dot{m}_{\text{out}} = \int_{y_0}^{y_j}\rho u\,\mathrm{d}y = \rho_2 u_2\int_{y_0}^{y_j}\frac{\rho}{\rho_2}\frac{u}{u_2}\mathrm{d}y = \frac{L}{\sigma}\rho_2 u_2(1-C_2^2)I_{1j}. \tag{14}$$

For continuity, one equates $\dot{m}_{\text{in}}$ and $\dot{m}_{\text{out}}$ to get,

$$C_2\frac{L}{\sigma h}I_{1j} = \frac{b_r}{h}J_{1r}C_r/\sqrt{(\lambda_r)}. \tag{15}$$

This equation is used to evaluate C_r.

2.7.2. *Conservation of momentum for CV-I.* Conservation of momentum for CV-I may be written as,

$$\int_0^1\frac{P-P_b}{P_b}\mathrm{d}\frac{y}{h} = \frac{2\gamma}{\gamma-1}C_r^2\frac{b_r}{h}J_{2r} \tag{16}$$

However, use of this equation required a base pressure distribution, $P = P(y/h)$, which is not generally known. For this reason, it was decided to develop a mechanical energy equation instead.

2.7.3. *Conservation of mechanical energy for CV-I.* A mechanical energy balance will now be written for Control Volume I in order to obtain L/h, the length of the shear or mixing layer. The following analysis is essentially that suggested by Korst [30] although the current derivation is similar to that of Hesler [55]. The mechanical energy balance may be expressed semantically as,

(Shear Work)$_{\text{in}}$ + (Net Kinetic Energy)$_{\text{in}}$ = (Total Dissipation).

The shear work consists of mechanical energy into the control volume because of shear forces along the dividing streamline. One may write the mechanical energy balance as,

$$\underbrace{\int_0^L\tau_j u_j\,\mathrm{d}x}_{ME\text{ shear}} + \underbrace{\frac{1}{2}\int_{y_0}^{y_j}\rho u^3\,\mathrm{d}y}_{ME\text{ in by bulk flow}} - \underbrace{\frac{1}{2}\int_0^{b_r}\tilde{\rho}\tilde{u}^3\,\mathrm{d}\tilde{y}}_{ME\text{ out by bulk flow}} = \underbrace{\int_{\text{vol}}e_d\,\mathrm{d}V.}_{\text{Total Dissipation}} \tag{17}$$

However, the total dissipation itself may be separated into components,

$$\int_{\text{vol}}e_d\,\mathrm{d}V = \Psi_{MZ}+\Psi_{RF}+\Psi_{BL}+\Psi_{\text{core}}. \tag{18}$$

An extremely long and detailed derivation in Appendix G of Smith [41] and elsewhere [56] provide analytical expressions for each of the terms in equations (17) and (18) as follows:

$$\dot{M}E_{\text{shear}} = (1-C_2^2)\rho_2 U_2^3 I_{2j}\varphi_j\frac{L}{\sigma} \tag{17a}$$

$$\dot{M}E_{\text{in}} = \tfrac{1}{2}b_r\tilde{\rho}_r\tilde{U}_r(1-C_r^2)J_{3r} \tag{17b}$$

$$\dot{M}E_{\text{out}} = \tfrac{1}{2}\frac{L}{\sigma}\rho_2 U_2^3(1-C_2^2)I_{3j} \tag{17c}$$

$$\Psi_{MZ} = \frac{\rho_2 U_2^3(1-C_2^2)I_{2j}L}{\sigma_c - \eta_j^2 2^{3/2}}\left[\operatorname{erf}[(\sqrt{2})\eta_j] - \operatorname{erf}[(\sqrt{2})\eta_0]\right] \tag{18a}$$

$$\Psi^{RF} = \tilde{\rho}_r \tilde{U}_r^3(1-C_r^2)\frac{\pi^2}{4}\int_{S_c}^{0} K\phi^3 \int_0^1 \frac{\tilde{\varphi}\sin^2(\pi\zeta)}{\tilde{\Lambda}\cdot TR}\zeta\, d\zeta\, ds \tag{18b}$$

$\Psi_{\text{core}} = 0$ since dissipation is hypothesized to be negligible in this quiescent zone. (18c)

Ψ_{BL} supplied in tabular form by separate code [56]. (18d)

The integrals are evaluated numerically while values of Ψ_{BL} are computed with a supersonic turbulent boundary layer code [56] and parameterized for insertion in PROGRAM NRWAKE as tabular data.

2.8. *Control volume II (CV-II)*

The nonisobaric control volume, shown in Fig. 1, includes the flow reversal region bounded by the dividing streamline, the flow centerplane, and the interface station. The interface station separates CV-I from CV-II and was selected physically as the beginning of recompression.

2.8.1. *Continuity for CV-II.* All mass entering this control volume, exited from CV-I. Conversely all mass leaving this control volume enters CV-I. Thus a mass balance on this control volume gives an equation which is identical to equation (15) or continuity for CV-I. As noted earlier, the continuity relation for CV-II is redundant and contributes no new information.

2.8.2. *Conservation of momentum for CV-II.* A momentum balance for the s-direction yields,

$$F_s - P_b h_r - P_b(y_j - y_0)\cos\alpha = \dot{M}_{\text{out}} + \dot{M}_{\text{in}}\cos\alpha. \tag{19}$$

A momentum balance for the y-direction yields,

$$F_y + P_b(y_j - y_0)\sin\alpha - (S_w - S_r)(P_b + P_w)\tfrac{1}{2} = -\dot{M}_{\text{in}}\sin\alpha. \tag{20}$$

The momentum flux out of CV-II is the momentum flux into CV-I and conversely so the expressions for momentum flux derived earlier are again applicable. Additionally, a geometric relationship,

$$F_s = F_y\tan\alpha, \tag{21}$$

is used to combine the two momentum component equations (19) and (20) into a single equation for the unknown wall pressure, P_w, at the point of dividing streamline reattachment.

$$\frac{P_w}{P_b} = 1 + \frac{2/(S_w - S_r)}{h}\sin\alpha\left(\frac{\dot{M}_{\text{out}}}{P_b h}\cos\alpha + \frac{\dot{M}_{\text{in}}}{P_b h}\right). \tag{22}$$

Using this expression for P_w, a quantity $N' = (P_w - P_b)/(P_1 - P_b)$ is defined which has been shown [25] to correlate pressure rise to reattachment with free stream Mach number much better than the N-factor suggested by Nash [9].

3. CLOSURE CONDITIONS FOR BASE PRESSURE

At this point, the flow component analysis is complete since all flow variables are known in terms of assumed values of base pressure, P_b. One now seeks a closure condition which will select the correct P_b for a given free stream Mach number, M_1. Basically the interaction between the outer inviscid flow and the inner viscous layer determines P_b. Since the Chapman–Korst escape criterion is well known, it will be discussed first and then used as a fiducial for comparison with the other approaches.

3.1. *Chapman–Korst escape criterion*

The separated flow must eventually realign itself with the downstream wall or flow centerline. This realignment of the external flow causes an adverse pressure gradient and streamlines which do not have sufficient kinetic energy to overcome or escape this adverse gradient and are reversed back into the near wake cavity. One streamline, which just stagnates at the wall, divides the flow which turns back and recirculates from that which has sufficient kinetic energy to escape or proceed downstream. For the case of zero mass bleed into the base region, this streamline is known by various names such as the dividing, discriminating, or stagnating streamline.

Korst postulated that the isentropic stagnation pressure along the dividing streamline (P_{0j}) must equal the maximum static pressure (P_4) downstream of the recompression region. Isentropic relations are assumed to be valid although the flow is known to be diabatic and irreversible. Thus the escape criterion asserts that $P_{0j} = P_4$ where for a plane wake $P_4 \approx P_1$. That is, in a plane wake, the upstream approach pressure is recovered. Thus,

$$\frac{P_1}{P_b} = \frac{P_{0j}}{P_b} = \left(\frac{T_{0j}}{T_j}\right)^{\gamma/(\gamma-1)} = \left(\frac{1}{1-C_j^2}\right)^{\gamma/(\gamma-1)}$$

$$\text{or} \quad \frac{P_b}{P_1} = \frac{P_2}{P_1} = (1-C_j^2)^{\gamma/(\gamma-1)}. \tag{23}$$

This key equation gives the Chapman–Korst prediction of base pressure which will be used as a fiducial. In the literature, discussion of the validity of the Chapman–Korst escape criterion makes no mention of C_j. It is clear from equation (23) that the Chapman–Korst pressure is a direct function of C_j and hence shear layer profile among other things. For this reason, it is somewhat meaningless to say that the Chapman–Korst criterion either over- or underpredicts a value without stating details about how C_j was obtained. This fallacy is repeated often in the literature.

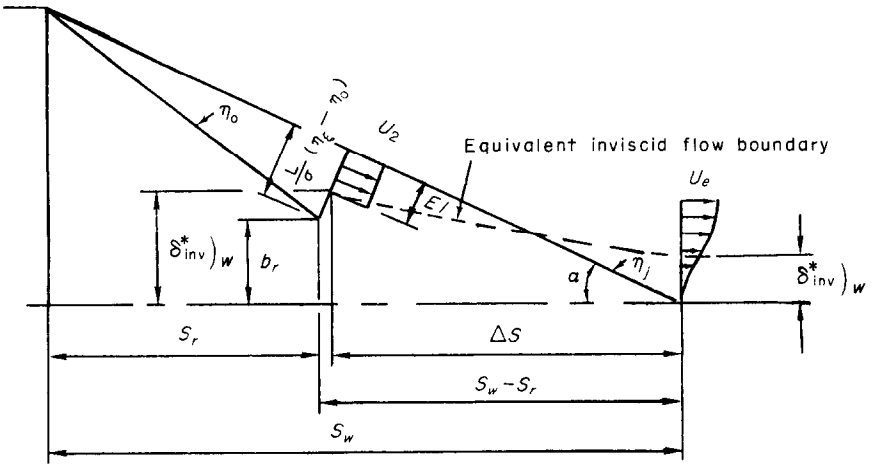

FIG. 2. Equivalent inviscid (EI) flow.

3.2. *Displacement thickness at reattachment*

In this section, the correct base pressure will be selected by matching viscous and inviscid estimates of displacement thickness, δ^*, at reattachment as proposed by Greenwood [31]. To obtain a viscous estimate, δ^*_v, of displacement thickness, one can use the reattachment profile derived in Section 2.5. By assuming negligible entrainment between the interface station and reattachment, continuity may be written as,

$$\int_{y_j}^{y_e} \rho u \, dy = \int_0^{\delta} \rho \hat{u} \, dy \tag{24}$$

where δ = boundary-layer thickness at reattachment and $\hat{u}$ is the velocity from the reattachment profile, equation (6). But

$$\int_{y_j}^{y_e} \rho u \, dy = \frac{L}{\sigma} \rho_2 u_2 \frac{T_2}{T_{02}} (I_{1e} - I_{1j}) = \frac{L}{\sigma} \rho_2 u_2 \frac{T_2}{T_{02}} I_{2r} \tag{24a}$$

and

$$\int_0^{\delta} \rho \hat{u} \, dy = \delta \rho_e U_e (1 - C_e^2) \int_0^1 \frac{\rho}{\rho_e} \frac{\hat{U}}{U_e} dZ$$

$$= \delta \rho_e U_e \frac{T_e}{T_{0e}} \hat{I}_{ie}. \tag{24b}$$

Inserting these expressions into equation (24), one may solve for δ. Using the usual definition of boundary-layer displacement thickness, one writes,

$$(\delta^*_{visc})_w = [1 - (1 - C_e^2) I_{1e}] \delta. \tag{25}$$

This completes the viscous estimate of δ^* at the reattachment station. Now one needs a corresponding inviscid estimate of δ^*. One can define an inviscid displacement height at the interface station as the height of the dividing streamline minus an equivalent inviscid flow width, EI, as shown in Fig. 2.

$$\rho_2 u_2 EI = \int_{y_0}^{y_j} \rho u \, dy = \rho_2 u_2 \frac{T_2}{T_{02}} \frac{L}{\sigma} I_{1j}$$

$$\text{or} \quad EI = (1 - C_2^2) \frac{L}{\sigma} I_{1j} \tag{26}$$

$$(\delta^*_{inv})r = b_r + \left[(\eta_j - \eta_0) \frac{L}{\sigma} - EI \right] \cos \alpha. \tag{27}$$

This is the distance from the wall or centerplane to the lower boundary of the equivalent inviscid slug at the cutoff station. To get δ^*_{inv} at reattachment, the change from the interface station to reattachment is required. Using a sequence of linear pressure changes to turn the flow from the interface station to the reattachment station as described in Smith [41], one writes,

$$\Delta S = S_w - S_r - \left[(\eta_j - \eta_0) \frac{L}{\sigma} - EI \right] \sin \alpha$$

$$\Delta \delta^* = \frac{\Delta S}{N} \sum_{\theta_2}^{\theta_e} \tan \theta_i \tag{28}$$

N is the number of turns, $\Delta\theta$, or pressure increments, ΔP.

$$(\delta^*_{inv})_w = (\delta^*_{inv})_r - \Delta \delta^*. \tag{29}$$

The value of P_b which causes the inviscid δ^*_i of equation (29) to equal the viscous δ^*_v of equation (25) is the correct P_b.

3.3. *Downstream throat width*

The Crocco–Lees critical point theory can be construed as indicating the existence of a downstream throat. The flow continues turning back toward the axial direction as it recompresses. Ultimately it again is

flowing parallel to the centerline (flow angle = θ_1) and reaches the free stream pressure, P_1. When this condition is first achieved the flow height will have reached its minimum throat height δ_t. It is possible to determine a value of P_b such that the viscous and inviscid estimates, $\delta_{t,v}$ and $\delta_{t,i}$, are equal.

Experiments indicate that pressure varies linearly from the interface station to reattachment and the downstream throat. Nevertheless a linear pressure increase will be used for simplicity to estimate the downstream throat station which is used in calculating the downstream throat width. This approximation is considered appropriate since the exact location of the throat is immaterial to the general calculation scheme. Only the width which is primarily a function of the pressure difference is important.

For a linear variation in pressure,

$$S_t = (S_w - S_{re}) \frac{1 - \dfrac{P_e}{P_1}}{\dfrac{P_e}{P_1} - \dfrac{P_2}{P_1}} + S_w. \tag{30}$$

One begins the calculation with the flow height, δ_e, at reattachment including the effect of transverse pressure gradient, $\partial P/\partial y$. The flow is allowed to turn in a sequence of small $\Delta\theta$'s from θ_e and P_e at reattachment to θ_1 and P_1 at the downstream throat. After summing the tangents of each θ_i, one finds,

$$\delta_{t,i} = \delta_e - \frac{(S_e - S_w)}{N} \sum_{\theta_e}^{\theta_1} \tan\theta_i. \tag{31}$$

As before, N equals the number of incremental turns, $\Delta\theta$, or number of incremental pressure changes, ΔP. Equation (31) furnishes the inviscid estimate of downstream throat width. A corresponding viscous estimate will be found from continuity applied to flow areas with unit dimension into the paper. The usual one-dimensional expression [48] is,

$$\frac{A}{A^*} = \frac{1}{M}\left[\frac{2}{\gamma+1}\left(1 + \frac{\gamma-1}{2}M^2\right)\right]^{(\gamma+1)/[2(\gamma-1)]}. \tag{32}$$

One evaluates this equation at reattachment where $A_e = \delta_e \cdot 1$ and at the downstream throat where $A_t = \delta_t \cdot 1$. Forming the ratio of the two resulting equations one finds,

$$\frac{\delta_t}{\delta_e} = \frac{M_e}{M_1}\left[\frac{1 + \dfrac{\gamma-1}{2}M_1^2}{1 + \dfrac{\gamma+1}{2}M_e^2}\right]^{(\gamma+1)/[2(\gamma-1)]} \tag{33}$$

Which can be written as,

$$\delta_{t,v} = \delta_e \frac{C_e}{C_1}\left(\frac{1 - C_e^2}{1 - C_1^2}\right)^{1/(\gamma-1)} \tag{33a}$$

This is the viscous estimate of downstream throat width which is to be matched against the corresponding inviscid estimate from equation (31).

3.4. *Mass flow rate per unit area at downstream throat*

Rather than determining P_b by matching the viscous and inviscid estimates of a particular field variable, this section is concerned with the possibility that there is a stationary point in the variation of the mass flow rate per unit area at the downstream throat versus base pressure. By assuming that the Crocco–Lees hypothetical nozzle analogy is literally true, one infers that the mass flow rate at reattachment is also valid at the downstream throat station. That is, the nozzle hypothesis rules out entrainment. The mass flow rate at reattachment is readily determined as follows:

$$\dot{m} = \int_0^{\delta_e} \rho u \, \mathrm{d}\bar{y} = \rho_e u_e \delta_e \int_0^1 \frac{\rho}{\rho_2}\frac{U}{U_e}\,\mathrm{d}Z \tag{34}$$

where $Z = \bar{y}/\delta_e$.

After considerable manipulation as detailed in Appendix J of [41] one finds,

$$\dot{m}/\rho_1 u_1 h/\delta_{t,\mathrm{avg}} = \frac{P_e}{P_1}\frac{TR_1}{\delta_{t,\mathrm{avg}}}\frac{C_e}{C_1}\frac{\delta_e}{h}\sqrt{(T_{01}/T_{0e})} \times \int_0^1 \frac{P}{P_e}\frac{\varphi\,\mathrm{d}Z}{\Lambda - C_e^2\varphi^2}. \tag{35}$$

Where $\delta_{t,\mathrm{avg}} = \frac{1}{2}(\delta_{ti} + \delta_{tv})$ is the average of the viscous and inviscid estimates of downstream throat width. Because of the unit depth in the planar configuration, this is also the average downstream throat area. Consequently equation (35) represents the mass flow rate per unit area at the downstream throat.

The integration in equation (35) is performed numerically after assuming a linear pressure variation.

$$\frac{P}{P_e} = \frac{P_w}{P_e} + Z\left(1 - \frac{P_w}{P_e}\right). \tag{36}$$

Where $P = P_e$ at $Z = 1$ and $P = P_w$ at $Z = 0$. The wall pressure, P_w, is obtained from a momentum balance on control volume II as discussed in Section 2.8.2. External pressure at the edge of the layer, P_e, is obtained from equation (4). Although, in principle, one could differentiate equation (35) with respect to P_b and determine the extrema, it is much easier in practice to merely assume values of P_b and find the stationary point graphically as follows: For computational ease, one merely computes and plots values of mass flux from equation (35) vs P_b. It is hypothesized that the correct P_b corresponds to the stationary point of the graph for each Mach number.

Table 3. Tabulated isoenergetic predictions

Closure scheme	M_1	M_2	$\frac{P_2}{P_1}$	$\frac{P_{\text{eff}}}{P_1}$	$\frac{P_w}{P_1}$	$\frac{P_e}{P_1}$	$\frac{N' \text{ or } P_w-P_2}{P_1-P_2}$	σ	$\frac{S_r}{h}$	$\frac{S_{re}}{h}$	$\frac{S_w}{h}$	$\frac{S_t}{h}$	$\frac{L}{h}$	$\left(\frac{L}{h}\right)_{\max}$	$\frac{\delta_r}{h}$	$\frac{\delta_e}{h}$	$\frac{\delta_t}{h}$	$\frac{\delta^*}{h}$
1. Escape criterion	1·5	1·96	0·50	0·53	0·79	0·78	0·56	13·4	1·80	1·90	3·81	5·17	1·93	2·10	0·67	0·37	0·32	0·17
2. Throat height	1·5	1·86	0·58	0·62	0·89	0·88	0·71	13·3	1·99	2·08	4·72	5·64	2·10	2·32	0·74	0·45	0·43	0·21
3. δ^* match	1·5	2·01	0·46	0·49	0·74	0·73	0·50	13·5	1·71	1·81	3·44	4·94	1·85	2·00	0·63	0·34	0·28	0·15
4. Min. mass flux	1·5	1·96	0·50	0·53	0·79	0·78	0·56	13·4	1·80	1·90	3·81	5·17	1·93	2·10	0·67	0·37	0·32	0·17
1. Escape criterion	2	2·67	0·35	0·38	0·68	0·65	0·46	14·4	1·64	1·74	3·03	4·30	1·80	1·91	0·57	0·31	0·24	0·14
2. Throat height	2	2·62	0·38	0·42	0·73	0·70	0·52	14·3	1·71	1·81	3·26	4·42	1·86	1·98	0·59	0·33	0·27	0·16
3. δ^* match	2	2·71	0·33	0·36	0·65	0·62	0·43	14·4	1·59	1·70	2·89	4·23	1·76	1·87	0·55	0·29	0·21	0·13
4. Min. mass flux	2	2·67	0·35	0·38	0·68	0·65	0·46	14·4	1·64	1·74	3·03	4·30	1·80	1·91	0·57	0·31	0·24	0·14
1. Escape criterion	3	4·14	0·20	0·23	0·53	0·50	0·37	16·4	1·66	1·76	2·79	4·26	1·83	1·90	0·49	0·26	0·17	0·13
2. Throat height	3	4·11	0·21	0·24	0·55	0·52	0·39	16·4	1·69	1·78	2·86	4·27	1·86	1·93	0·50	0·27	0·18	0·14
3. δ^* match	3	4·14	0·20	0·23	0·53	0·50	0·37	16·4	1·66	1·76	2·79	4·26	1·83	1·90	0·49	0·26	0·17	0·13
4. Min. mass flux	3	4·11	0·21	0·24	0·55	0·52	0·39	16·4	1·69	1·78	2·86	4·27	1·86	1·93	0·50	0·27	0·18	0·14
1. Escape criterion	4	5·71	0·13	0·16	0·43	0·41	0·32	18·6	1·80	1·89	2·88	4·73	1·97	2·01	0·45	0·25	0·13	0·13
2. Throat height	4	5·64	0·14	0·17	0·46	0·44	0·35	18·5	1·83	1·92	2·97	4·72	2·00	2·04	0·47	0·26	0·15	0·14
3. δ^* match	4	5·58	0·15	0·18	0·49	0·47	0·38	18·4	1·87	1·95	3·06	4·72	2·03	2·07	0·48	0·26	0·16	0·14
4. Min. mass flux	4	5·58	0·15	0·18	0·49	0·47	0·38	18·4	1·87	1·95	3·06	4·72	2·03	2·07	0·48	0·26	0·16	0·14
1. Escape criterion	5	7·40	0·09	0·11	0·36	0·34	0·27	20·6	1·97	2·06	3·05	5·36	2·14	2·16	0·43	0·23	0·10	0·13
2. Throat height	5	7·27	0·10	0·13	0·40	0·38	0·31	20·5	2·01	2·10	3·16	5·31	2·18	2·19	0·44	0·24	0·12	0·14
3. δ^* match	5	6·98	0·13	0·17	0·50	0·48	0·40	20·1	2·13	2·20	3·48	5·22	2·27	2·30	0·48	0·28	0·18	0·16
4. Min. mass flux	5	7·07	0·12	0·15	0·46	0·44	0·39	20·2	2·09	2·17	3·37	5·25	2·24	2·26	0·47	0·27	0·16	0·15

4. RESULTS AND COMPARISON TO EXPERIMENTAL DATA

4.1. *General comments*

Isoenergetic results and comparisons to experimental data will now be presented. Nonisoenergetic results are omitted here for brevity but are presented in Smith [41].

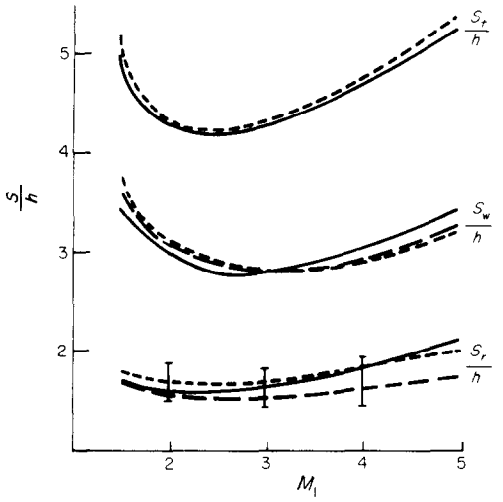

FIG. 3. Location of recompression, S_r, reattachment of dividing S, L, S_w, and downstream throat station, S_t, vs approach Mach number, M_1. ———, Greenwood [17]; ———, Present study based on throat height; – – – –, Present study based on minimum mass flux; |, range of data from Roshko and Thomke [23] and Hama [26].

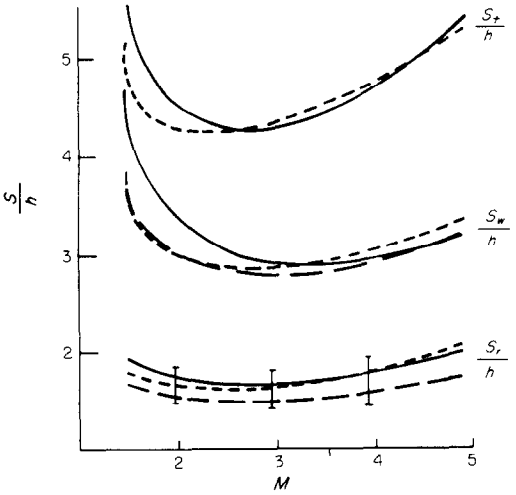

FIG. 4. Location of recompression, S_r, reattachment of dividing S, L, S_w, and downstream throat station, S_t, vs approach Mach number, M_1. ———, Greenwood [17]; ———, Present study based on throat height; – – – –, Present study based on minimum mass flux; |, range of data from Roshko and Thomke [23] and Hama [26].

4.2. *Results*

Table 3 is a tabulation of many predicted parameters by the four closure schemes for five values of Mach number. Graphs of certain key predictions along with experimental data are presented as a measure of prediction accuracy.

Figures 3 and 4 illustrate the variation of three crucial axial stations with approach Mach Number. The three axial stations in question locate (1) the beginning of recompression (or interface between control volumes), S_r, (2) the reattachment point of the dividing streamline, S_w, and (3) the location of the hypothetical downstream throat, S_t. Figure 3 shows results of the two already known closure schemes, the escape criterion and the δ^*-match. Figure 4 shows results of the two new closure methods; the throat height match and the minimum mass flux method. For comparative purposes, Greenwood's [31] predictions of S_r and S_w and the experimental data band for S_r from Roshko and Thomke [32] and Hama [1] are shown on both figures.

Three of the four closure schemes in this study, the escape criterion and the two viscous and inviscid matches of throat and displacement thickness, provide a ratio which passes through unity as the correct value of pressure is attained. Only the fourth method based on a stationary point in the graph of mass flux per unit throat area versus base pressure as in Fig. 5 provides an interesting and even surprising plot. This method begins with an arbitrary initial value of P_b which is then incremented while computing corresponding values of mass flux with equation (35). An analogy with the usual one-dimensional isentropic flow from gas dynamics indicated that a maximum mass flux per unit area might be expected. Instead a minimum in the curve for each Mach number correctly predicts a unique base pressure which is in close agreement with experimental data. Even with hindsight, it is difficult to explain this behavior. However, the close agreement with experiment over a broad Mach number range in addition to the agreement with the other three prediction methods rules out fortuitous agreement.

4.3. *Comparison of isoenergetic results to experimental data*

Regardless of the fundamentally sound theoretical basis of the present analysis, only by comparison to experimental data can one validate the results. Figure 6 compares experimental data to base pressure predictions by each of the four closure schemes for various approach Mach numbers.

Some experimenters are not explicitly clear about whether the pressure measured is purely static or has a dynamic component. In [41], actual base pressure vs approach Mach number for the four closure schemes is plotted and observed to compare more closely with

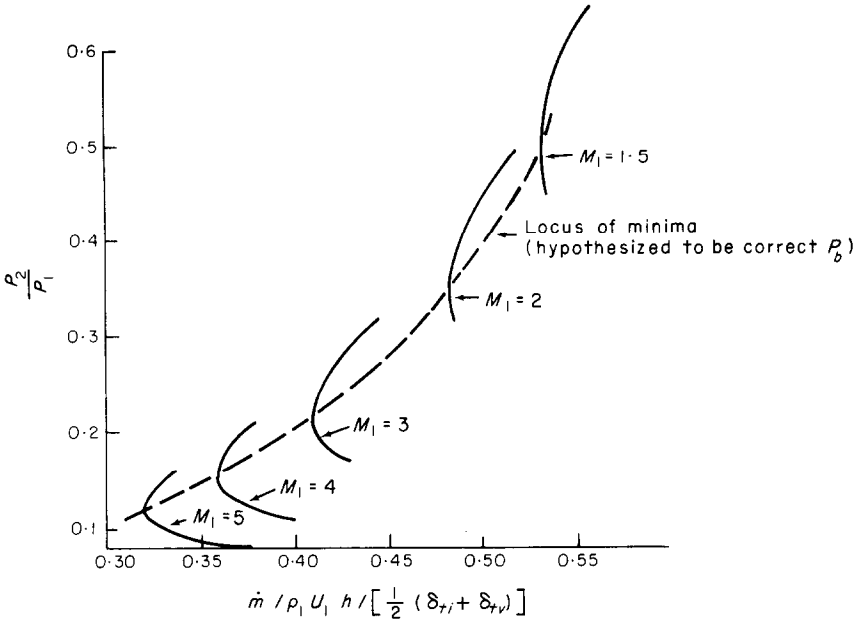

FIG. 5. Base pressure vs mass flux for fixed Mach number.

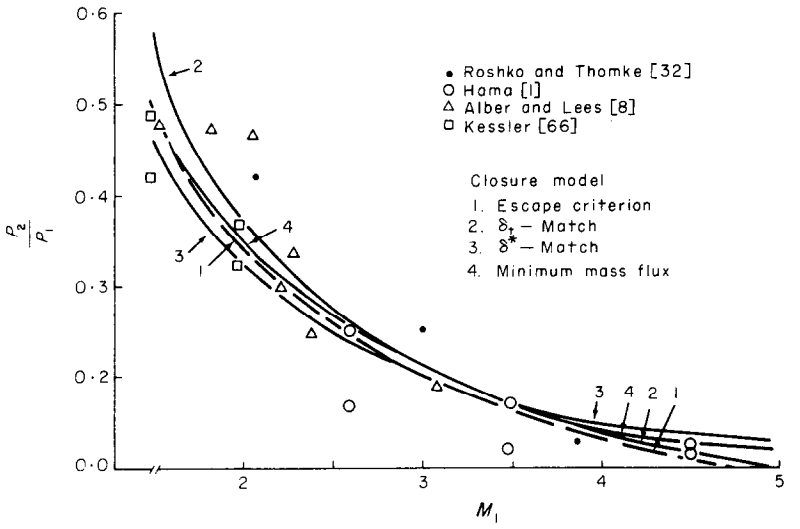

FIG. 6. Comparison of base pressure predictions to experimental data with four closure methods.

experimental data than does an effective base pressure containing a component of dynamic pressure.

Figure 7 presents the longitudinal wall pressure distribution for Mach 3 showing both the current predictions and representative experimental data. Similar plots for lower and higher Mach numbers are contained in Smith [41]. Slopes of the pressure–position lines agree with data trends for all methods and all Mach numbers. However, the predicted values of the critical stations, S_r, S_w, and S_t are slightly low at Mach 2, slightly high at Mach 4, and just right at Mach 3 [41]. For the present study, this represents an adequate compromise. If improvement is desired, Lamb and Hood [39] demonstrated the efficacy of an empirical lip shock correction.

Figure 8 gives a measure of reattachment pressure predictions versus experimental data. The ratio $(P_w - P_b)/(P_1 - P_b)$ has been shown to be a good correlating parameter by Hood [25]. Hood's calculations are shown as a dashed line in Fig. 8. An

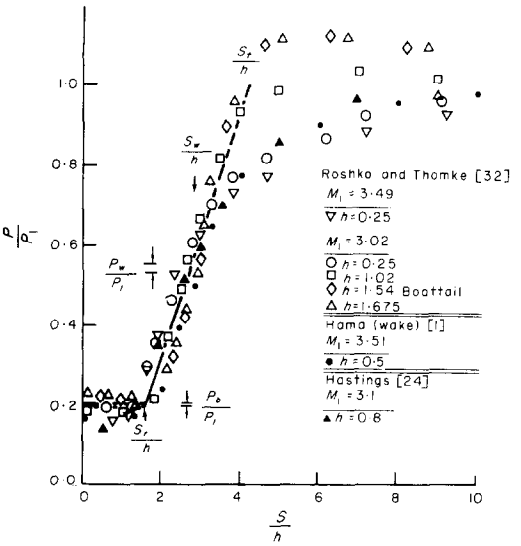

FIG. 7. Comparison with experimental pressure distributions for $M_1 \approx 3$.

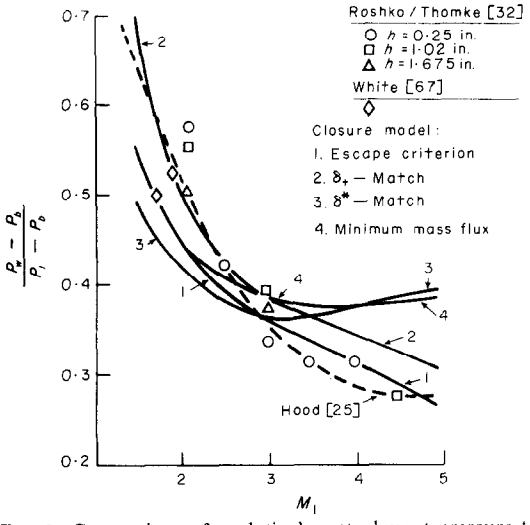

FIG. 8. Comparison of analytical reattachment pressure to experimental data.

interesting observation is that although Hood used the escape criterion for prediction of base pressure, his results differ from the present escape criterion predictions at low Mach numbers. This comparison demonstrates the sensitivity of this closure scheme to the shear layer velocity profile shape and hence the dividing streamline velocity.

5. SUMMARY

5.1. *Comparison of present models to others in literature*

The results presented in Section 4 indicate that the supersonic turbulent base flow techniques derived herein are satisfactory for engineering predictions. Each of the prediction methods developed herein accounts for the strong interaction of the outer inviscid flow with the inner viscous region. One method, the now classical Chapman–Korst escape criterion, is used as a fiducial for comparisons to the others since it is known to exhibit correct trends. Another closure model is an improved version of one, which originated in the earlier work of Greenwood [31], and consists of matching viscous and inviscid estimates of displacement thickness at the point of dividing streamline reattachment.

The two completely new closure models proposed in this study represent a marriage of the hitherto separate avenues of effort within the last two decades. The Chapman–Korst advocates have emphasized simplicity and ease of use while the Crocco–Lees proponents have achieved a greater wealth of details and accuracy although admittedly with time consuming complexity. The present approach is eclectic. The simple Chapman–Korst component analysis is used for arbitrary base pressure and the Crocco–Lees critical point or hypothetical downstream throat method is used to select the correct base pressure. The proposed new methods are as simple to use as the Chapman–Korst component analysis, but they are also based on the widely accepted Crocco–Lees concept. None of the objectionable assumptions of the Chapman–Korst escape criterion concerning isentropic flow are required in the present models. As far as is known, a merger of the Chapman–Korst and Crocco–Lees methods has not been attempted before.

The two original methods mentioned above are based upon extending the Crocco–Lees downstream throat analogy to include well-known attributes of one-dimensional gas dynamics. One approach consists of matching viscous and inviscid estimates of the hypothetical downstream throat width. The final closure method uses the fact that, at a critical flow condition, the variation of mass flux per unit area at the hypothetical downstream throat possesses a stationary point. In the present study, it is hypothesized that the correct P_b is the base pressure which causes the mass per unit area at the downstream throat to pass through a stationary point which is a minimum.

Alber and Lees [8] mention that Korst [3], Nash [9], and others are concerned primarily with base pressure and treat the recompression process as a black box. Alber and Lees [8] further point out that such theories are deficient in that they ignore the all important viscous-inviscid interaction. As a result, they say that theories of this type cannot predict such important wake characteristics as the length of recompression zone, $(S_t - S_r)$, the location of the rear stagnation point, S_w, growth rate of the wake boundary layer, $d\delta/dS$, and longitudinal pressure variation in the reattachment region, dP/dS. The present study remedies every one of these objections albeit in an approximate manner.

Readers who are accustomed to extremely accurate and detailed calculations may believe erroneously that these approximations are too crude to be of value. Indeed the present author's previous experience has been concerned primarily with very accurate and time-consuming finite difference techniques [57, 58]. Even so, it soon became clear that the present integral techniques, approximate profiles, and linear variations are as accurate as knowledge of crucial input quantities will allow. The present weak links lie in the understanding of the physics such as knowledge of profiles, turbulent transport properties, etc. These limitations would defeat any attempt at surpassing the engineering accuracy achieved herein.

5.2. *Final closure and future extensions*

The general utility of the present method of analysis stems from the short development time and ease of use. The computer code NRWAKE developed here performs four complete base flow analyses for each Mach number in less than 20 seconds CPU time on the CDC 6600. Normally one will use only one of the closure methods, thus decreasing the run time per Mach number significantly. In contrast to the current approach, many very detailed difference methods require years of development. Their usage can require double precision accuracy to locate the critical point and many minutes per computer simulation. Even if extensive details and accuracy are warranted, the present methods will prove valuable as a precursor to a detailed method. In a typical design study, many parametric analyses are required to isolate final design candidates which are worthy of more detailed analysis.

It is known (for example see Hood [25]) that the flow field is but little affected by moderate heat transfer. Hence, the energy equation may be uncoupled from the motion equations. Heat-transfer predictions may be added to the present flow field calculations by using global energy balances in the control volumes as in Lamb and Hood [26]. As partial confirmation, Larson's experiments [59] show that T_0 in the separated zone is only 5 per cent less than in the free stream, even for highly cooled walls; so wall temperature probably has little effect on pressure distribution. A more difficult addition in the future will be consideration of the upstream boundary layer. Possibly a supersonic turbulent boundary layer code developed earlier [56] can be used in conjunction with the present code.

REFERENCES

1. F. R. Hama, Experimental studies on the lip shock, *AIAA Jl* **6**, 212–219 (1968).
2. D. R. Chapman, An analysis of base pressure at supersonic velocities and comparison with experiment, NACA TN-2137 (July 1950).
3. H. H. Korst, A theory for base pressures in transonic and supersonic flow, *Trans. Am. Soc. Mech. Engrs* **78**, 593–600 (1956).
4. L. Crocco and L. Lees, A mixing theory for the interaction between dissipative flows and nearly isentropic streams, *J. Aeronaut. Sci.* **19**, 649–676 (1952).
5. G. B. Schubauer and P. S. Klebanoff, Investigation of the separation of the turbulent boundary layer, NACA Report 1030 (1951).
6. R. H. Korkegi, Survey of viscous interactions associated with high Mach number flight, *AIAA Jl* **19**(5), 771–784 (May 1971).
7. L. G. Hunter and B. L. Reeves, Results of a strong interaction, wake-like model of supersonic separated and reattaching turbulent flows, *AIAA Jl* **9**(4), 703–712 (April 1971).
8. I. E. Alber and L. Lees, Integral theory for supersonic turbulent base flow, *AIAA Jl* **6**, 1343–1351 (1968).
9. J. F. Nash, An analysis of two-dimensional turbulent base flow, including the effect of the approaching boundary layer, National Physical Laboratory, AERO Report 1036 (30 July, 1962).
10. H. McDonald, Turbulent shear layer reattachment with special emphasis on the base pressure problem, *Aeronaut. Q.* **15**, 247–280 (1964).
11. W. H. Webb, R. J. Golik, F. W. Vogenitz and L. Lees, A multimoment theory for the laminar supersonic near wake, in *Proceedings of the 1965 Heat Transfer and Fluid Mechanics Institute*. Stanford University (1965).
12. B. L. Reeves and L. Lees, Theory of the laminar near wake of blunt bodies in hypersonic flow, *AIAA Jl* **3**(11), 2061–2074 (November 1965).
13. E. Baum, An interacting model of a supersonic laminar boundary layer near a sharp backward facing step, TRW Systems, BSD TR 67–81 (1966).
14. E. Baum and M. R. Denison, Interacting supersonic laminar wake calculations by a finite difference method, *AIAA Jl* **5**, 1224–1230 (1967).
15. S. J. Shamroth and H. McDonald, A new solution of the turbulent near-wake recompression problem, AIAA Paper No. 20-228 (1970).
16. R. Weiss and S. Weinbaum, Hypersonic boundary-layer separation and the base flow problem, *AIAA Jl* **4**, 1321–1330 (1966).
17. M. S. Holden, Theoretical and experimental studies of the shock wave-boundary layer interaction on curved compression surfaces, in *Proceedings of the Symposium on Viscous Interaction Phenomena in Supersonic and Hypersonic Flow*, Aerospace Research Labs, Wright–Patterson Air Force Base, Ohio (May 1969).
18. L. Crocco, Considerations on the shock-boundary layer interaction, in *Proceedings of the Conference on High Speed Aeronautics*, Polytechnic Institute of Brooklyn, pp. 75–112 (January 1965).
19. F. N. Kirk, An approximate theory of base pressure in two-dimensional flow at supersonic speeds, Royal Aeronautical Establishment, TN Aero 2377 (1959).
20. J. B. Roberts, On the prediction of base pressure in two-dimensional supersonic turbulent flow, National Gas Turbine Establishment Report R265 (November 1964); also issued as Aeronautical Research Council R&M 3434 (1966).
21. J. C. Cooke, Separated supersonic flow, Royal Aeronautical Establishment, TN Aero 2879 (March 1963).
22. J. M. Wu, M. W. Su and M. G. Scherberg, Experimental investigation of supersonic flow separation over a rearward facing step, AIAA Paper No. 70-106 (1970).

23. H. E. Smith, The flow field and heat transfer downstream of a rearward facing step in supersonic flow, Aerospace Research Laboratories Report No. 67-0056 (March 1967).
24. R. C. Hastings, Turbulent flow past two-dimensional bases in supersonic streams, Royal Aircraft Establishment, TN Aero 2931 (December 1963).
25. C. G. Hood, A multi-stage integral analysis of diabatic turbulent separated regions in planar supersonic flow, Ph.D. Dissertation, University of Texas at Austin (June 1968).
26. J. P. Lamb and C. G. Hood, An integral analysis of turbulent reattachment applied to plane supersonic base flows, *J. Engng. Ind.* **90B**, 553–560 (1968).
27. A. Martellucci and C. J. Studerus, Ballistic vehicle drag for offensive weapons systems, *J. Defense Res. Ser. A: Strategic Warfare* **2A**(1), 120–166 (Spring 1970).
28. J. M. Cassanto, Effect of cone angle and bluntness ratio on base pressure, *AIAA Jl* **3**(12), 2351 (December 1965).
29. J. M. Cassanto and E. M. Storer, A revised technique for predicting the base pressure of sphere–cone configurations in turbulent flow, including mass addition effects, AFM 68-41, General Electric RS (October 1968).
30. H. H. Korst, Dynamics and thermodynamics of separated flow, in *Proceedings—Symposium, Single and Multi-Component Flow Processes*, Rutgers Engineering Research Publ. No. 45 (1965).
31. T. F. Greenwood, An integral model for the turbulent, supersonic near-wake employing strong interaction concepts, Ph.D. Dissertation, University of Texas at Austin (December 1971).
32. A. Roshko and G. J. Thomke, Observations of turbulent reattachment behind and axisymmetric downstream-facing step in supersonic flow, *AIAA Jl* **4**, 975–980 (1966).
33. M. G. Johnson, Predictions of planar turbulent supersonic base flows including mass bleed and diabatic effects, M.S. Thesis, University of Texas at Austin (May 1969).
34. M. E. Childs, G. C. Paynter and E. Redeker, The prediction of separation and reattachment flow characteristics for two-dimensional supersonic and hypersonic turbulent boundary layers, *AGARD Conference Proceedings No. 4: Separated Flows*, pp. 325–352 (May 1966).
35. T. J. Kessler and R. H. Page, Supersonic turbulent boundary layer separation ahead of a wedge, *Proceedings of the 10th Midwestern Mechanics Conference* (1967).
36. R. H. Page, T. J. Kessler and W. G. Hill, Jr., Reattachment of two-dimensional supersonic turbulent flows, ASME Paper 67-F-20 (1967).
37. J. L. Stollery and W. L. Hankey, Subcritical and supercritical boundary layers, *AIAA Jl* **8**(7), 1349–1351 (July 1970).
38. J. Erdos and A. Pallone, Shock-boundary layer interaction and flow separation, *Proceedings Heat Transfer and Fluid Mechanics Institute* (1962).
39. J. P. Lamb and C. G. Hood, Prediction of heat-transfer rates downstream of a backstep in supersonic turbulent flow, ASME Paper No. 70-HT/SpT-39 (1970).
40. W. D. Hayes and R. F. Probstein, *Hypersonic Flow Theory*, Vol. 1, *Inviscid Flows*. Academic Press, New York (1959).
41. J. H. Smith, Development and comparison of several analytical models for the planar turbulent near wake in supersonic flow combining component and critical point methods, Ph.D. Dissertation, University of Texas at Austin (1973).
42. J. P. Lamb, An approximate theory for developing turbulent shear layers, *J. Bas. Engng* **89D**, 633–642 (1967).
43. J. L. Gaddis, An analytical study of gaseous film cooling, Ph.D. Dissertation, University of Texas at Austin (1968).
44. R. C. Bauer, An analysis of two-dimensional laminar and turbulent compressible mixing, *AIAA Jl* **4**(3), 392–395 (March 1966).
45. R. S. Channapragada and N. P. Wooley, Turbulent mixing of parallel compressible free jets, AIAA Paper 65-606 (1965).
46. D. C. Reda and R. H. Page, Supersonic turbulent flow reattachment downstream of a two-dimensional backstep, AIAA Paper No. 70-108 (1970).
47. J. P. Lamb, C. G. Hood and M. G. Johnson, A convective transport model for turbulent supersonic planar base flow, ASME Paper No. 70-HT/SpT-35 (1970).
48. A. H. Shapiro, *The Dynamics and Thermodynamics of Compressible Fluid Flow*, Vols. I and II. The Ronald Press, New York (1954).
49. W. L. Chow, Recompression of a two-dimensional supersonic turbulent free shear layer, *Proceedings of the Twelfth Midwestern Mechanic Conference*, University of Notre Dame, Indiana, 16–18 August (1971).
50. H. Schlichting, *Boundary-Layer Theory*, 6th Edn, pp. 193–194. McGraw-Hill, New York (1968).
51. G. Maise and H. McDonald, Mixing length and kinematic eddy viscosity in a compressible boundary layer, *AIAA Jl* **6**, 73–80 (January 1968).
52. J. J. Schauer and R. H. Eustis, The flow and heat transfer characteristics of plane turbulent impinging jets, Stanford University, Department of Engineering, Tech. Report No. 3 (1963).
53. M. Wolfshtein, Some solutions of the plane turbulent impinging jet, *J. Bas. Engng* **92D**(4), 915–922 (December 1970).
54. C. E. Peters, Turbulent mixing and burning of coaxial streams inside a duct of arbitrary shape, Arnold Engineering Development Center, Report No. AEDC-TR-68-270 (January 1969).
55. L. J. Hesler, A unified analysis of planar and axisymmetric turbulent near wakes in supersonic flow, Ph.D. Dissertation, University of Texas at Austin (1972).
56. J. P. Lamb, L. J. Hesler and J. H. Smith, A generalized integral computation technique for nonequilibrium compressible turbulent boundary layers using moment equations, *J. Appl. Mech.* **94E**, 667–672 (September 1972).
57. J. H. Smith, Modification of radiant enclosure equations for third generation digital computers, *J. Spacecraft Rockets* **7**(12), 1492–1494 (December 1970).
58. J. H. Smith, Survey of three-dimensional finite difference forms of heat equation, Sandia Laboratories Report SC-M-70-83 (March 1970).
59. H. K. Larson, Heat transfer in separated flow, *J. Aeronaut. Sci.* **26**(11), 731–738 (1959).
60. D. K. Ai, On the critical point of the Crocco–Lees mixing theory in the laminar near wake, *J. Engng Maths* **4**(2), 169–182 (April 1970).
61. S. Weinbaum and R. W. Garvine, An exact treatment of the boundary layer equations describing the two-dimensional viscous analog of the one-dimensional inviscid throat, AIAA Paper No. 68-102 (1968).
62. H. H. Korst, R. H. Page and M. E. Childs, A theory for

base pressure in transonic and supersonic flow, University of Illinois, Engineering Experiment Station, ME-TN-392-2 (March 1955).
63. D. R. Chapman, D. M. Kuehn and H. K. Larson, Investigation of separated flows in supersonic streams with emphasis on the effects of transition, NACA TN 3869 (March 1957).
64. R. H. Page and R. J. Dixon, Base heat transfer in a turbulent separated flow, Fifth International Symposium of Space Technology, Tokyo (July 1963).
65. T. F. Greenwood, An analytical study of the base flow problem including the theories of Korst, Zumwalt and Nash, Report No. IM-AA-3-65-8, Brown Engineering Co., Inc., Huntsville, Alabama (March 1965).
66. T. J. Kessler, A theory for two-dimensional supersonic turbulent base flows, AIAA Paper 69-68 (1969).
67. R. A. White, Turbulent boundary layer separation from smooth convex surfaces in supersonic two-dimensional flow, Ph.D. Dissertation, University of Illinois (1963).

UNIFICATION DES APPROCHES DE CROCCO–LEES ET DE CHAPMAN–KORST RELATIVES AU PROCHE SILLAGE

Résumé—Après avoir présenté les deux approches classiques, on résout par les techniques intégrales le problème de l'écoulement turbulent de culot ($1{,}5 \leqslant M_\infty \leqslant 5$). On fusionne les deux branches séparées que sont l'analyse de Chapman–Korst et la méthode du point critique de Crocco–Lees. On supprime la dichotomie en utilisant l'analyse de Chapman–Korst pour établir tous les paramètres d'écoulement en fonction des valeurs de la pression de culot. Une fermeture est obtenue en prenant deux interprétations de la théorie de Crocco–Lees pour choisir la pression de culot correcte. Le fait que les méthodes de calcul et les mesures expérimentales sont en bon accord, donne une solide confiance en ces méthodes nouvelles.

AUSGEWÄHLTE ZUSAMMENFASSUNG DES CROCCO–LEES UND DES CHAPMAN–KORST-ANSATZES FÜR GEBIETE IN DER NÄHE DER WIRBELZONE

Zusammenfassung—Neben einem Überblick über die beiden klassichen Ansätze wird das Problem der turbulenten ebenen Überschall-Grundströmung ($1{,}5 \leqslant M_\infty \leqslant 5$) auf eine neue Art mit Integral-Techniken gelöst. Die bis jetzt unterschiedlichen Lösungsbemühungen der Chapman–Korst-Komponentenanalyse und der Crocco–Lees-Methode des kritischen Punktes werden zusammengefaßt. Die Aufspaltung wird beendet durch Benutzen der Chapman–Korst-Komponentenanalyse zur Darstellung aller Strömungsparameter in Termen angenommener Werte des Bodendrucks. Ein Zusammenschluß wird dann durch Verwendung zweier Interpretationen der Crocco–Lees-Theorie des kritischen Punktes zur Wahl des korrekten Bodendrucks entsprechend den interessierenden Parametern erreicht. Die Tatsache der guten Übereinstimmung der Vorherbestimmungsmethoden mit umfassenden experimentellen Daten liefert eine wesentliche Bestätigung der neuen Methoden.

СОВМЕСТНОЕ ПРИМЕНЕНИЕ МЕТОДОВ КРОККО–ЛИСА И ЧЕПМАНА–КОРСТА ДЛЯ РАССМОТРЕНИЯ БЛИЖНЕГО СЛЕДА

Аннотация — В статье, помимо описания двух классических методов, новым интегральным методом решается задача сверхзвукового ($1{,}5 \leqslant M_\infty \leqslant 5$) турбулентного плоского донного течения. В работе объеденены до сих пор раздельно существующие методы, базирующиеся на компонентном анализе Чепмана–Корста и методе критических точек Крокко–Лиса. Компонентный анализ Чепмана–Корста используется для выражения всех параметров течения через принятые величины давления у основания. Оба метода совмещаются путём использования двух вариантов теории критических точек Крокко–Лиса для выбора правильного давления у основания и соответствующих параметров течения. Тот факт, что результаты расчёта хорошо согласуются с многочисленными экспериментальными данными, говорит в пользу новых методов.